10.24425/acs.2024.153103

Archives of Control Sciences
Volume 34(LXX), 2024
No. 4, *pages* 805–831

Internal model control based sliding mode controller design for unstable second order delayed processes with a case study on CSTR

Mohammed Hasmat ALI and Md Nishat ANWAR

Controlling the unstable processes is challenging since one or more poles are located on the right side of the s-plane. The existence of dead time in these systems makes control much more difficult. In this paper, internal model control based sliding mode control has been proposed for the control of unstable processes with dead time. Two sliding surfaces based on PID and PIDPI are used to design of the proposed controller. The parameters of continuous and discontinuous control law are obtained using differential evolution optimization technique. An objective function is constituted in terms of performance measure (integral absolute error) and control effort measure (total variation of controller output). Illustrative examples demonstrate the superiority of the proposed controller over earlier reported work in this realm, especially in terms of load disturbance rejection. A case study on temperature management of a continuous stirred tank reactor during an irreversible exothermic process also serves to highlight the applicability of the proposed system. Furthermore, robustness of the proposed controller is also investigated by inclusion of perturbations in the parameters. The obtained results clearly show how well the suggested controller works.

Key words: internal model control, sliding mode, unstable processes, second order with dead-time processes, CSTR

1. Introduction

The internal model control (IMC) structure is shown in Fig. 1, which contains the process model. If the model is perfect, the IMC-based system becomes open-loop. On the other hand, if the model-mismatch is found, the error between the plant and model outputs is used as feedback signal to compensate the mismatch. The robustness is achieved by using a proper filter for model-mismatch case

Mohammed Hasmat Ali (corresponding author, e-mail: hashmatalig@gmail.com) and Md Nishat Anwar are with Department of Electrical Engineering, National Institute of Technology Patna, India.

Received 17.05.2023.

in IMC design [1]. Using the IMC technique, the complexity of the controller depends only on the complexity of the model and the required performance by the user.

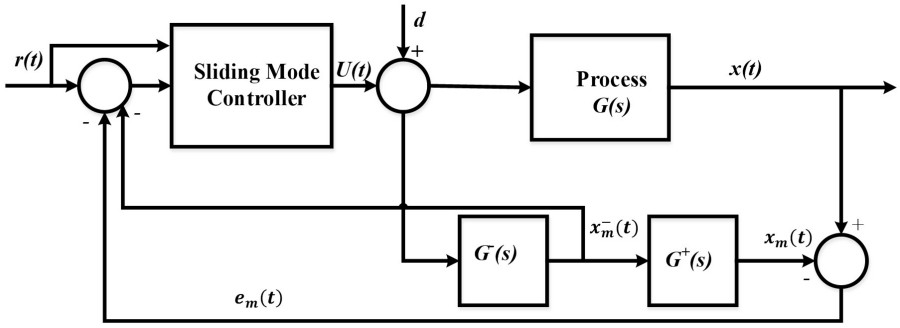

Figure 1: IMC based SMC scheme

The sliding mode control (SMC) is best known for its robustness to modelling errors of the plant and unknown disturbances. Its suitability is well proven for nonlinear and time-varying systems [2]. With these properties, SMC is widely used in various applications like chemical industry [3–6], robotics [7], process control [8,9], aerospace [10,11], power system [12,13], ocean engineering [14,15] and biomedical processing [16,17]. The main objective of sliding mode controller (SMCr) design is to move the system from its initial state to a selected surface on which the process can slide to its desired value. SMCr design has two steps: one is to define a sliding surface and the other is to design a control law that steers the states of the system to that surface as quickly as possible.

In the past two decades, researchers of process control industry focused attention to application of SMC for the control of industrial processes [3,5,8,18–23]. Some researchers [8, 19, 20] have used simple SMC structure to design first order plus dead-time (FOPDT) based plant model with small time delay and their performance degrades when applied to delay dominant processes. For the performance improvement in case of complex processes, the SMC has been applied with modified control structures like IMC and Smith predictor (SP) [5,18,21–23]. Talange *et al.* [22] have presented IMC based SMC to improve the performance and robustness of a temperature-flow cascade control system. Parte *et al.* [23] have utilized generalized predictive control (GPC) with SMC to control FOPDT process model. Camacho *et al.* [24] have proposed internal model control scheme-based SMCr (IMC-SMCr) for large ratio of dead-time (t_0) and time-constant (τ). Their method was based on FOPDT model and the controller parameters were obtained using the Nelder–Mead search algorithm. Camacho and Cruz [21] have proposed SP-based SMC for first order integrating process with large dead-time. Mehta and

Kaya [18] have proposed an SP based SMC for large dead-time process where improved load-disturbance response have been achieved using a meta-heuristic algorithm namely particle-swarm optimization technique. A dynamic SMCr with modified SP has been developed by Herrera *et al.* [3] for long dead-time process with inverse response dynamics. Espin *et al.* [5] have proposed a modified SP-based SMC for delayed integrating process. The methods of [3] and [5] were based on FOPDT process model and may be applicable to higher order process by approximating them to FOPDT one.

All the schemes reported above, give a SMCr with modified control structures for stable processes only. Mehta and Rojas [25] have given SP based SMC for delay dominant unstable FOPDT processes with improved load-disturbance response. In their work, the parameter of the controller has been obtained using metaheuristic cuckoo-search algorithm.

Works related to the application of SMC with modified control structures in the process industry are listed in Table 1. It is observed from the table that most of the researchers have presented SMCr design with different structures for FOPDT process only.

However, an approximated FOPDT model is not enough to describe the dynamics for higher order unstable plants as there may be suppression of some information in the plant apart from unstable dynamic lags. Hence, a second order plus dead-time (SOPDT) model would be a better choice for unstable plants for representing an unstable higher order plant because it draws more useful information regarding plant dynamics over FOPDT model. In this work, IMC based SMCr is proposed for the first time to control unstable SOPDT processes. Two different sliding surfaces with five and seven control parameters are used for designing purpose of the proposed controller to achieve a satisfactory closed loop system performance. The control parameters are obtained from the set of tuning equations using SOPDT model and a recent metaheuristic algorithm namely differential evolution (D-E) optimization technique. Extensive examples are simulated to present the merits of the proposed method over some recent methods reported in the literature. The main contributions of this paper are as follows:

- The IMC-SMCr is proposed with a new sliding surface and excellent set-point tracking as well as load-disturbance rejection responses are achieved.
- The IMC-SMCr is designed for unstable processes based on SOPDT model instead of FOPDT model.
- The proposed controller gives better control performance even in perturbed conditions.
- The suggested scheme's implementation is demonstrated by a presentation case study on CSTR temperature regulation.

Table 1: A review on SMC with modified control structure in process control

Literature	Process model used	Modified structure considered	Type of sliding surface taken	Continuous control law ($u_c(t)$)	Method of finding continuous control law	Discontinuous control law ($u_d(t)$)	Method of finding discontinuous control law
Talange *et al.* [26]	Stable FOPDT	IMC based SMC	PI	$\frac{\tau}{K}\left[\frac{y(t)}{\tau}+\lambda e(t)\right]$	Using Nelder-Mead search algorithm	$k\tanh\left(\frac{s(t)}{\Omega}\right)$	Using Nelder-Mead search algorithm
Parte *et al.* [23]	Stable FOPDT	SMC with GPC	PID	$\frac{1}{K}X(k)+\frac{(t_0+\tau)^2}{4Kt_0\tau}e(k)$	From tuning equation and fitting technique	$K_D\frac{s(t)}{\lvert s(t)\rvert+\eta}$	From tuning equation and fitting technique
Camacho [27]	Stable FOPDT	SMC with Smith predictor (SP)	P	$\left(\frac{t_0\tau}{K}\right)\left[\frac{X(t)}{t_0\tau}+\lambda_0 e(t)\right]$	From tuning equations having dead-time, gain and time constant	$K_D\frac{s(t)}{\lvert s(t)\rvert+\delta}$	From tuning equations having dead-time, gain and time constant
Mehta and Kaya [18]	Stable FOPDT	SMC with SP	PI	$\left(\frac{1}{k_m}\right)\left[\tau_m\lambda e(t)+y_m^-(t)\right]$	Using PSO optimization technique	$\alpha\lvert S(t)\rvert^{\beta}\,\mathrm{sign}(S(t))$	Using PSO optimization technique
Camacho *et al.* [24]	Stable FOPDT	SMC with IMC	PI	$\left(\frac{\tau}{K}\right)\left[\frac{dR(t)}{dt}+\frac{x_m^-(t)}{\tau}+\lambda e(t)\right]$	Using Nelder-Mead search algorithm	$K_D\frac{s(t)}{\lvert s(t)\rvert+\delta}$	Using Nelder-Mead search algorithm
Herrera *et al.* [3]	Stable FOPDT	SMC with SP	PI	$\left(\frac{1}{2k_m(\lambda-\eta)}\right)\left[(-\lambda_m\tau_m t_0+2\tau_m+t_0)Y^*+\lambda_m\tau_m t_0 e^*(t)+2Y^*-2k_m U_{DSMC}(t)\right]$	From tuning equations obtained for crirtical or overdamped system	$K_D\mathrm{sgn}(\sigma)$	From tuning equations obtained for a crirtical or overdamped system

Table 1 [cont.]

Literature	Process model used	Modified structure considered	Type of sliding surface taken	Continuous control law ($u_c(t)$)	Method of finding continuous control law	Discontinuous control law ($u_d(t)$)	Method of finding discontinuous control law
Mehta and Rojas [25]	Unstable FOPDT	SMC with SP	PI	$\left(\frac{1}{k_m}\right)\left[\tau_m\lambda e(t) + y_m^-(t)\right]$	Using cuckoo search optimization technique	$\alpha\,\lvert S(t)\rvert^{\beta}\,\mathrm{sign}(S(t))$	Using cuckoo search optimization technique
Camacho and Cruz [21]	ISOPDT	SMC with SP	PID	$\left(\frac{1}{K}\right)\left[(1-\tau_m\lambda_1)\frac{dX_1(t)}{t_0\tau} + \tau_m\lambda_0 e(t)\right]$	From controllability relationship	$K_D\frac{s(t)}{\lvert s(t)\rvert+\delta}$	Nelder-Mead search algorithm
Espin [5]	IFOPDT	SMC with SP	PID	$\left(\frac{1-\lambda_1\tau}{kt_f}\right)\frac{dx_1(t)}{dt} + \left(\frac{\lambda_0}{kt_f}\right)e(t) - \frac{m(t)}{t_f}$	From tuning equation and fitting technique	$K_D\,\mathrm{sgn}(S(t))$	From tuning equation and fitting technique
Morales [6]	FOPDT	Hybrid SMC with AI and IM	PI	$\frac{1}{K}x_t(t) + \frac{\lambda\tau}{K}x_t(t)e(t)$	Using Nelder-Mead search algorithm	$K_D\frac{s(t)}{\lvert s(t)\rvert+\delta}$	Using Nelder-Mead search algorithm
Proposed[1]	Unstable SOPDT	SMC with IMC	PID	$\left(\frac{1}{K}\right)\left[\dot{x_m^-}(t)\,(bk_3-ak_1) - x_m^- + ak_2/k_3\{(r(t)-x_m(t)-e_m(t))\}\right]$	Using DE algorithm	$K_D\frac{s(t)}{\lvert s(t)\rvert+\delta}$	Using DE algorithm
Proposed[2]	Unstable SOPDT	SMC with IMC	PIDPI	$\left(\frac{1}{k_3K}\right)\left[\dot{x_m^-}(t)\,(bk_3-ak_1) + (ck_3-ak_2)\,x_m^- + (ak_2+ak_5)r(t) - \{ak_4\,(\dot{x_m}(t)+\dot{e_m}(t)) + ak_5(x_m(t)+e_m(t))\}\right]$	Using DE algorithm	$K_D\frac{s(t)}{\lvert s(t)\rvert+\delta}$	Using DE algorithm

This paper is organized as follows: Section 2 presents the fundamentals of IMC and SMCr to be used. The proposed IMC-SMCr design procedure is given in Section 2. Section 3 provides the objective function and optimization technique. Section 4 shows simulation results of the proposed method and comparison with recently reported methods. Finally, some conclusions are presented in Section 5.

2. IMC based SMCr design for unstable SOPDT

Internal Model Control Structure. The classical IMC structure is shown in Fig. 1, where $G(s)$ is the process, $G_M(s)$ is the process model. In IMC design method, the process model is factored into two parts as:

$$G_M(s) = G^-(s)G^+(s), \tag{1}$$

where, $G^+(s)$ and $G^-(s)$are the parts of the model that are non-invertible (i.e. containing the right-hand side zeros and the dead-time) and invertible (i.e. remaining part of the process model), respectively.

The IMC controller is designed using only invertible part of the model which simplifies controller design. The non-invertible part like dead-time of the process model is not taken into account for the controller design and hence does not require any assumption for the dead-time.

Sliding mode control. In this paper, one sliding surface, $S_1(t)$ with five control parameters is considered which is PID controller and a new sliding surface $S_2(t)$ with seven control parameters is proposed which is a PIDPI controller.

$$S_1(t) = k_1 e_1(t) + k_2 \int_0^t e_2(t)\,\mathrm{d}t + k_3 \frac{de_1(t)}{dt}, \tag{2}$$

$$S_2(t) = k_1 e_1(t) + k_2 \int_0^t e_1(t)\,\mathrm{d}t + k_3 e_2(t) + k_4 \int_0^t e_2(t)\,\mathrm{d}t + k_5 \frac{de_1(t)}{dt}. \tag{3}$$

Here e_1 is the error between reference input $r(t)$ and model output without delay $x_m^-(t)$, e_2 is the error between reference input $r(t)$ and plant output $x(t)$ and k_1, k_2, k_3, k_4, and k_5 are the tuning parameters which determine the performance of the system on the sliding surface. The aim of control is to bring the controlled variable be equal to its reference value at all the time, which means that error and its derivative must be zero. As the reference value is reached, Eq. (1) indicates that $s(t)$ becomes a constant value which means that $e(t)$ is zero at $t > 0$. To

maintain $s(t)$ at a constant value, it is desired to make

$$\frac{dS_1(t)}{dt} = k_1\frac{de_1(t)}{dt} + k_2e_2(t) + k_3\frac{d^2e_1(t)}{dt^2} = 0, \tag{4}$$

$$\frac{dS_2(t)}{dt} = k_1\frac{de_1(t)}{dt} + k_2e_1(t) + k_3\frac{d^2e_2(t)}{dt^2} + k_4e_2(t) + k_5\frac{d^2e_1(t)}{dt^2} = 0. \tag{5}$$

Once the sliding surface of SMC technique is decided, the control law $U(t)$ is to be developed which guarantees the controlled variable be equal to its reference value all the time and satisfies (4) and (5). Control law has two additive parts: first one is continuous control law $U_c(t)$ and second is discontinuous control law $U_d(t)$. Hence,

$$U(t) = U_c(t) + U_d(t). \tag{6}$$

Continuous control law is given by:

$$U_c(t) = f\left(x(t), r(t), x_m^-(t)\right). \tag{7}$$

The discontinuous control law, $U_d(t)$ is responsible for deriving the system towards the sliding surface. The discontinuous control law is discontinuous across sliding surface. This control law is a nonlinear switching element like ideal relay or saturation relay. In practical, it is very difficult to implement high switching control using these relays because of the presence of finite delays and physical limitation of actuators. It may produce chattering across the sliding surface which is highly undesirable [18]. Chattering is a high frequency oscillation across the sliding surface which can excite high frequency dynamics that are neglected in modelling of the system. To reduce the chattering, one technique is to choose the following sigma function for $U_d(t)$ as shown below [4],

$$U_d(t) = K_D\frac{s(t)}{|s(t)| + \delta}, \tag{8}$$

where K_D is a tuning parameter which is responsible for reaching the sliding mode. δ is tuning parameter which is responsible for reducing the chattering phenomenon. Now, to design the continuous control law part, consider an unstable SOPDT process model defined by the transfer function as

$$G(s) = \frac{X(s)}{U(s)} = \frac{Ke^{-ls}}{(\tau_1 s + 1)(\tau_2 s - 1)}, \tag{9}$$

where $X(s)$ is the output of the system, $U(s)$ is the input to the plant, K is the gain of the plant, l is delay of the plant and τ_1 and τ_2 are time constants. The process model can be written as:

$$G^-(s) = \frac{K}{(\tau_1 s + 1)(\tau_2 s - 1)}, \tag{10}$$

$$G^{+}(s) = e^{-ls}. \tag{11}$$

Since IMC scheme is designed using invertible part i.e. $G^{-}(s)$ only hence, the $G^{-}(s)$ will be considered as process model while designing the IMC-SMCr. Eq. (10) may be written in rational form as:

$$G^{-}(s) = \frac{X_m^{-}(s)}{U(s)} = \frac{K}{as^2 + bs - 1}, \tag{12}$$

where $a = \tau_1\tau_2$, $b = \tau_1 + \tau_2$.

Eq. (12) may be written in differential form as:

$$a\ddot{x}_m^{-}(t) + b\dot{x}_m^{-}(t) - x_m^{-}(t) = Ku(t). \tag{13}$$

For Proposed Surface $S_1(t)$

Solving Eq. (4) for the highest order differential term, Eq. (4) may now be written as

$$\begin{aligned}\frac{dS_1(t)}{dt} &= k_2 r(t) - k_2 x_m(t) - k_2 e_m(t) - k_1 \dot{x}_m^{-}(t) \\ &\quad - \frac{k_3}{a}\left(Ku(t) - b\dot{x}_m^{-}(t) + x_m^{-}(t)\right) = 0,\end{aligned} \tag{14}$$

where, $e_1(t) = r(t) - x_m^{-}(t)$ and $e_2(t) = r(t) - x_m(t) - e_m(t)$. Control law $u(t)$ can be obtained from Eq. (14) as:

$$u(t) = \frac{\dot{x}_m^{-}(t)\,(bk_3 - ak_1) - x_m^{-} + ak_2/k_3\{(r(t) - x_m(t) - e_m(t))\}}{K}. \tag{15}$$

In sliding mode control technique, the control law $u(t)$ depends on continuous control law, $u_c(t)$ only, when the system reaches the sliding surface. Hence, $u_c(t)$ may be expressed as

$$u_c(t) = \frac{\dot{x}_m^{-}(t)\,(bk_3 - ak_1) - x_m^{-} + ak_2/k_3\,(r(t) - x_m(t) - e_m(t))}{K}. \tag{16}$$

From Eqs. (6), (15) and (16), control law $U_1(t)$ may be written as:

$$\begin{aligned}U_1(t) &= \frac{\dot{x}_m^{-}(t)\,(bk_3 - ak_1) - x_m^{-} + ak_2/k_3\,(r(t) - x_m(t) - e_m(t))}{K} \\ &\quad + K_D\frac{S_1(t)}{|S_1(t)| + \delta},\end{aligned} \tag{17}$$

where

$$S_1(t) = \mathrm{sgn}(K)\left(k_1 e_1(t) + k_2\int_0^t e_2(t)\,\mathrm{d}t + k_3\frac{de_1(t)}{dt}\right). \tag{18}$$

A signum function, $\mathrm{sgn}(K)$ in Eq. (17) is added for proper functioning of controller [18]. The action of controller which never switches as $\mathrm{sgn}(K)$, depends only upon the gain of the plant [28].

For Proposed Surface $S_2(t)$

By following similar steps as in previous case, control law $U_2(t)$ may be found as:

$$U_2(t) = \frac{\dot{x}_m^-(t)\,(bk_3 - ak_1) + (ck_3 - ak_2)\,x_m^- + (ak_2 + ak_5)r(t)}{k_3 K} - \frac{ak_4\,(\dot{x}_m(t) + \dot{e}_m(t)) + ak_5(x_m(t) + e_m(t))}{k_3 K} + K_D \frac{S_2(t)}{|S_2(t)| + \delta}, \tag{19}$$

where

$$S_2(t) = \mathrm{sgn}(K)\left(k_1 e_1(t) + k_2 \int_0^t e_1(t)\,\mathrm{d}t + k_3 e_2(t) + k_4 \int_0^t e_2(t)\,\mathrm{d}t + k_5 \frac{de_1(t)}{dt}\right). \tag{20}$$

The overall control laws $U_1(t)$ and $U_2(t)$ will be determined by solving Eqs. (17) and (19), respectively. In this paper, their solution is obtained using an optimization technique D-E by minimising objective function comprising suitable performance indices. D-E is a stochastic, robust, easy to use and population-based optimization algorithm for solving nonlinear optimization problem. D-E technique converges faster and with certainty and requires few control variables [29]. The reason to prefer this optimization technique is that D-E algorithm has given better performance over other well-known optimization techniques viz. grasshopper optimization technique, cuckoo search, particle swarm optimization, genetic algorithm, ant colony, fire-fly algorithm [9, 29–31]. A detailed study of D-E optimization technique can be found in [32].

3. Selection of the objective function

The proper selection of the objective function is very important as it is responsible for better performance of the controller. The controller's performance is assessed on overshoot, settling time and load disturbance rejection etc. The controller which is designed with lesser integral absolute error (*IAE*) gives improved

response with less overshoot [33]. So, *IAE* is considered as a performance measure for formulation of objective function in this paper. The *IAE* is the integral of error signal and defined as

$$IAE = \int_0^\infty |e(t)| \, \mathrm{d}t, \tag{21}$$

where $e(t)$ is the error signal. *IAE* evaluates the output control performance by minimising its value. The controller designed using *IAE* performance index, may not be enough for claiming the optimum control input signal variations. To evaluate the manipulated input signal variation, total variation (*TV*) of input is computed which is sum of variations in control input $u(t)$. It is difficult to define *TV* for a continuous signal, but if the input signal is discretized as a sequence, $[u_1, u_2, \ldots, u_i, \ldots]$, it is defined as [33]

$$TV = \sum_{i=1}^{\infty} |u_{i+1} - u_i| \, . \tag{22}$$

TV should be as small as possible for minimal variation in input $u(t)$. It offers smoothness in the signal [33]. For optimizing error signal with minimum controller output signal variation, both the performance indices with required condition viz. minimal *IAE* value and minimum *TV* value are taken into account for making the objective function to find the optimal values of control parameters. Hence the objective function is defined as

$$J_{IAE,TV} = w_1 \int_0^\infty |e(t)| \, \mathrm{d}t + w_2 \sum_{i=1}^{\infty} |u_{i+1} - u_i| \, , \tag{23}$$

where w_1 and w_2 are the weight factors assigned to *IAE* and *TV*, respectively. In this paper, weight of 10% is assigned to *IAE* performance index while 90% weight is assigned to *TV* performance index. More weightage (90%) is given to *TV* as the SMC design has the chattering problem which results from dynamic control law.

D-E optimization technique is used to minimise the selected objective function to find the optimal values of control parameters. MATLAB 18a (2018) on Windows 10 with processor Intel i5 and RAM 8GB is utilized to perform the simulation using this technique. Simulation is run for 100 iterations which were sufficient to find the optimum control parameters for the required optimization problem.

4. Simulations

In this section, the proposed IMC-SMC technique has been validated through various examples along with a case study on a non-linear model of CSTR. Results obtained from the proposed techniques of IMC-SMC are compared in terms of the set-point and the load-disturbance responses for nominal and perturbed systems with the results obtained from recently reported methods. The results show the superiority of the proposed techniques especially in terms of fast settling time and load-disturbance (LD) rejection. The controller's effort of the proposed technique is compared with recent methods and it is found to be better. A comparison of performance indices *IAE*, Integral square error (*ISE*), integral time absolute error (*ITAE*) and *TV* for each example is shown in Table 2.

Example 1 (A process with an unstable pole)

An unstable SOPDT process is taken from literature given by Siddiqui *et al.* [9]. They have shown the improved results over the results obtained from previous studies done by Mehta and Rojas [25] and Atic and Kaya [34]. The example is described by following transfer function as:

$$G_1(s) = \frac{e^{-0.5s}}{(2s-1)(0.5s+1)}. \tag{24}$$

The control parameters obtained through the proposed IMC-SMCr technique with PID (method 1) and PIDPI (method 2) surfaces are found to be ($k_1 = 25.0168$, $k_2 = 5.8811$, $k_3 = 8.4245$, $K_D = 4.6387$, $\delta = 7.0459$), ($k_1 = -24.1851$, $k_2 = -53.8543$, $k_3 = -44.2286$, $k_4 = -0.2495$, $k_5 = 10.3578$, $K_D = -1.4155$, $\delta = 19.1386$), respectively. Siddiqui *et al.* [9] have found the controller parameters as $k_1 = 2$, $k_2 = 0.45$, $k_3 = 3.5$, $K_D = 12.38$, $\delta = 2.69$ by their method. With these parameters, process is simulated and the process output and the controller output are shown in Fig. 2 and Fig. 3, respectively. It is observed from Fig. 2 that the proposed method 1 gives faster response for set-point change as compared to the method of Siddiqui *et al.* [9]. The set-point response is enhanced with the set-point filter. The set-point filter has been selected as proposed by Anwar and Pan [35]. There is significant improvement in the LD rejection response by the proposed techniques as LD response settles 8s earlier than the method of Siddiqui *et al.* [9]. It is also observed from Fig. 2 that process output undershoot in LD response is lowered by only 5% and 38% in the proposed method 1 and method 2, respectively, while the same is lowered by 100% in the method of Siddiqui *et al.* [9]. Furthermore, the process response by the method of Siddiqui *et al.* [9] is more oscillatory as compared to that from the proposed techniques.

The controller effort is vital in any closed-loop control system. Fig. 3 clearly shows that the control effort of the proposed methods outperform the method

Table 2: Performance indices

Method	Controller type	Nominal system								Perturbed system							
		Set-point response				Load response				Set-point response				Load response			
		IAE	*ISE*	*ITAE*	*TV*	*IAE*	*ISE*	*ITAE*	*TV*	*IAE*	*ISE*	*ITAE*	*TV*	*IAE*	*ISE*	*ITAE*	*TV*
Example 1																	
Proposed 1	IMC-SMC	0.9	94.3	–4.4	1	0	1.5	25.7	0.14	1.2	94.3	–5.7	1	0.32	0	1.48	0.14
Proposed 2	IMC-SMC	1	95.6	–0.8	1	1.1	0.28	3.7	0	1.2	95.6	–1.9	1	1.1	0.26	–4.07	0
Siddiqui *et al.* [36]	SMC	8.2	1.7	335.9	1363.9	12.7	5.45	406	740.3	18.5	5.8	767	895.1	23.12	8.81	1005	556.6
Example 2																	
Proposed 1 $*F_a$	IMC-SMC	0.47	14.1	–0.11	0.51	0.14	0	0.8	0.05	0.54	14.1	–0.5	0.51	0.14	0	0.8	0.05
Proposed 2 $*F_a$	IMC-SMC	0.39	13.9	1.08	0.5	0.24	0	–1.7	0	0.41	13.8	0.64	0.5	0.24	0	–1.8	0
Raza and Anwar $*F_b$ [36]	PID	1.23	0.09	12.67	5.09	0.57	0.05	2.2	2.38	1.3	0.1	12.78	27.19	0.62	0.05	3	12.5
Example 3																	
Proposed 1 $*F_c$	SMC	3.12	188	21.3	0.12	0.43	0	3.4	0.12	3.6	188	–28.14	0.12	0.45	0	3.4	0.12
Proposed 2 $*F_d$	SMC	2.41	196.2	9.7	1	0.39	0	3.5	0.11	3.62	196.2	18.51	1.06	0.39	0	4	0.13
Seer and Nandong $*F_e$ [36]	PID	9.26	2.25	188.9	6	7.1	1.7	123.2	6	15.8	3.2	812.3	6	10.62	2	474	6

*Set-point filters are $F_a = \frac{1}{(2.5s+1)}$, $F_b = \frac{1.49s^2+2.44s+1}{9.65s^2+2.7s+1}$, $F_c = \frac{1}{5.25s+1}$, $F_d = \frac{1}{(4s+1)}$, $F_e = \frac{1}{(8s+1)}$.

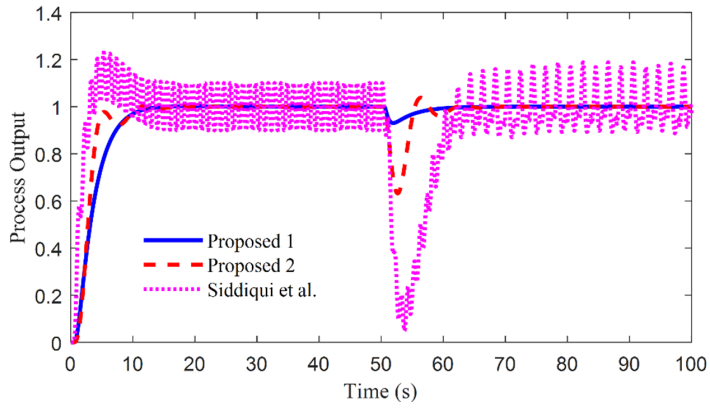

Figure 2: Process output of Example 1

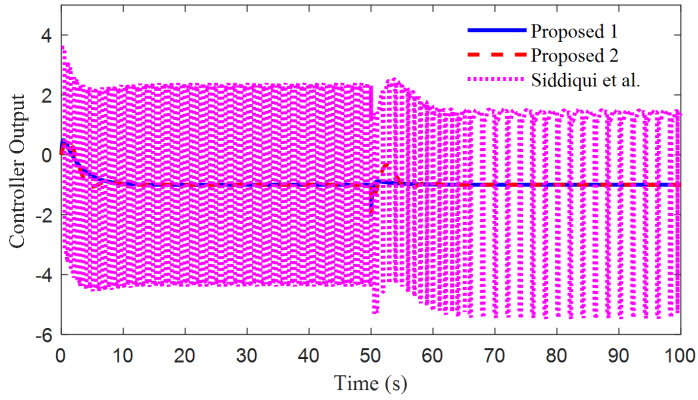

Figure 3: Controller output of Example 1

of Siddiqui et al. [9]. The performance indices *IAE, ITAE, ISE* and *TV* of the proposed methods and that of Siddiqui *et al.* [9] are shown in Table 2. A lower value of *IAE, ITAE, ISE*, and *TV* by the proposed methods is observed from Table 2, which shows the superiority of the proposed methods.

For robustness analysis, perturbation of +40% in delay (l) of the nominal process is introduced. The process output and the controller output for perturbed process by the proposed methods of IMC-SMCr and the method of Siddiqui *et al.* [9] are shown in Fig. 4 and Fig. 5, respectively. It is evident from Fig. 4 that the closed-loop performance is more robust by the proposed method. The smooth controller response in Fig. 5 and lesser value of *TV* from Table 2 indicates that the controller effort is smaller by the proposed method. It is also observed from Table 2 that integral errors *IAE, ISE* and *ITAE* for the proposed method is lesser

than Siddiqui *et al.* [9]. Hence, it may be concluded that the proposed method gives quite satisfactory result for both nominal and perturbed systems.

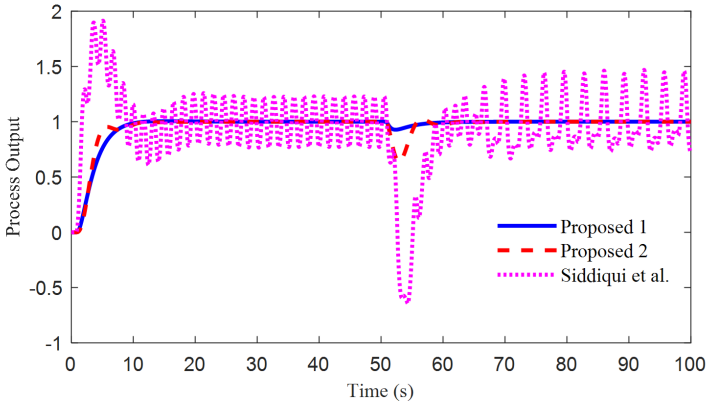

Figure 4: Process output of Example 1 for perturbed model

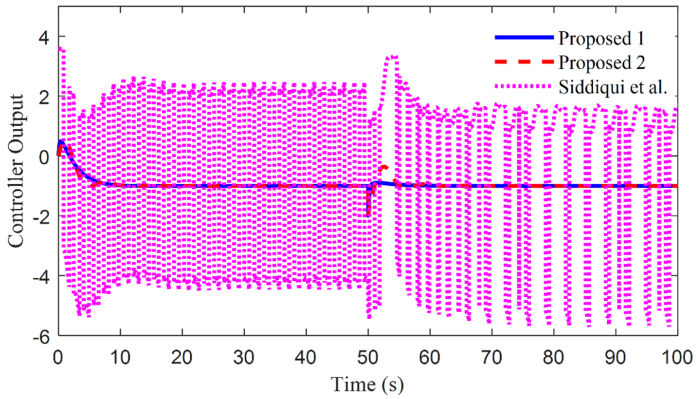

Figure 5: Controller output of Example 1 for perturbed model

Example 2 (A process with two unstable poles)

Example of $G_2(s)$ is an unstable SOPDT which is studied by Raza *et al.* [36], Cho *et al.* [37] and Shamsuzzoha and Lee [38]. The results obtained from the method of Raza *et al.* [36] are better than [37] and [38].

$$G_2(s) = \frac{e^{-0.2s}}{(3s-1)(s-1)}. \tag{25}$$

Raza *et al.* [36] have designed PID controller for the above process and the control parameters are $K_p = 2.39$, $K_i = 0.87$, $K_d = 8.49$ while the controller parameters

from the proposed IMC-SMC techniques with PID and PIDPI surfaces is found to be ($k_1 = 4.8835, k_2 = 2.8735, k_3 = 19.5147, K_D = 1.7615, \delta = 1.4792,$) ($k_1 = -5.2796, k_2 = -5.5991, k_3 = -1.78, k_4 = .6242, k_5 = -0.7436, K_D = -8.8673, \delta = 8.1242$), respectively. The responses for process output and controller output are shown in Fig. 6 and Fig. 7, respectively, and the figures clearly show that the responses for the proposed methods are better than Raza *et al.* [36] especially in LD rejection.

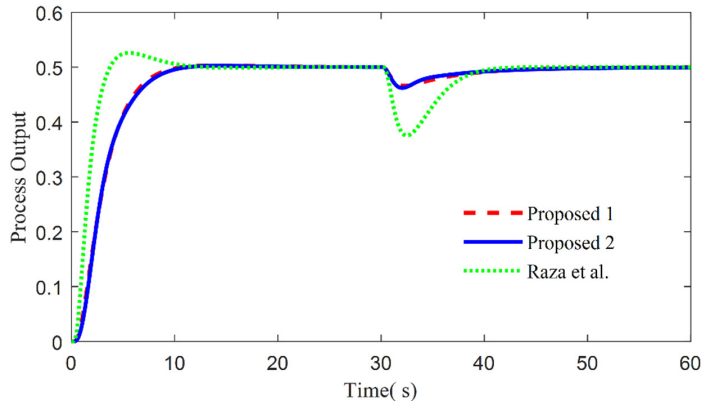

Figure 6: Process output of Example 2

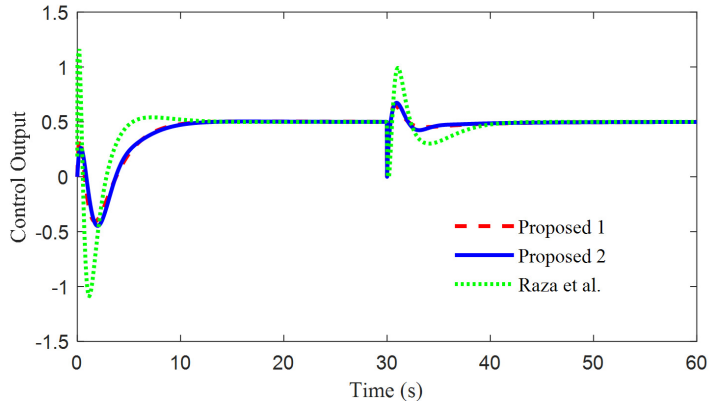

Figure 7: Controller output of Example 2

The process is also simulated for perturbation change of 10% in gain and 5% in dead-time simultaneously with same tuning parameters to check the robustness of the proposed technique. The process response of set-point and disturbance change for perturbed system are shown in Fig. 8 and Fig. 9, respectively, and

the figures clearly show that the process output and controller response for the proposed methods outperforms the method of Raza *et al.* [36]. The performance indices for the perturbed system for the proposed methods and the method of Raza *et al.* [36] are shown in Table 2. The table shows that *IAE, ISE* and *ITAE* values are lower for the proposed methods of both nominal and perturbed systems.

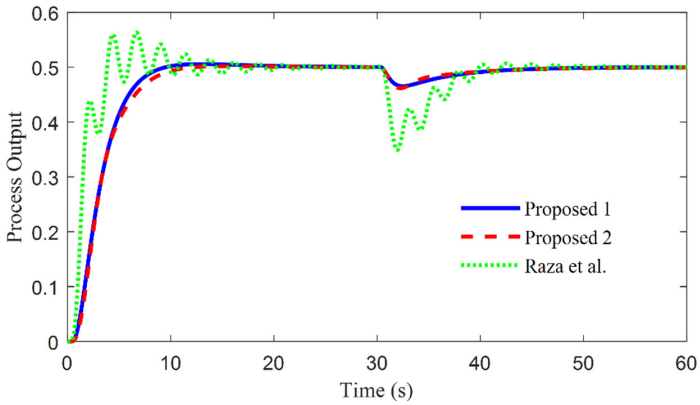

Figure 8: Process output for perturbed condition in Example 2

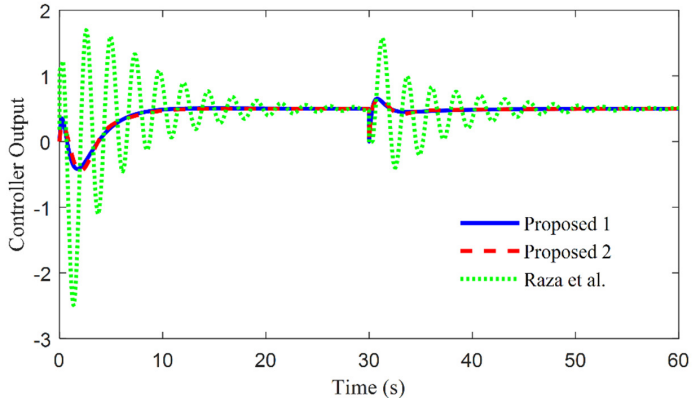

Figure 9: Controller output for perturbed condition in Example 2

Example 3 (Process with one unstable pole)

The suggested IMC-SMC is applied to an unstable process, [39]

$$G_3(s) = \frac{e^{-s}}{(3s-1)(10s+1)}. \tag{26}$$

By using the proposed IMC-SMC tuning methods based PID and PIDPI surfaces, controller parameters are obtained as ($k_1 = 11.27$, $k_2 = 1.75$, $k_3 = 17.13$,

$K_D = 5, \delta = 3$) and ($k_1 = 1.29, k_2 = -8.08, k_3 = -6.08, k_4 = -0.6, k_5 = 4.73, K_D = -4.7, \delta = 4.73$), respectively.

Seer and Nandong [39] have used PID tuning and obtained gains are $k_p = 3.2$, $k_i = 0.15, k_d = 23.4$. The process responses and controller efforts of the suggested techniques and method of [39] are displayed in Fig. 10 and Fig. 11. It is evident from the figures that the suggested PID and PIDPI surface based IMC-SMC techniques outperform the method of [39] in terms of improved set-point tracking and enhanced LD rejection. Furthermore, the error values (*IAE* and *ITAE*) and *TV* values for the proposed schemes are lower than [39] which shows the efficacy of the proposed schemes. To evaluate the robustness of the controllers, perturbation of +50% in K is introduced in the systems. Figure 12 and Fig. 13 display the responses of perturbed condition. It is clear from the figure that the suggested IMC-SMC techniques give better responses as compared to the method of [39].

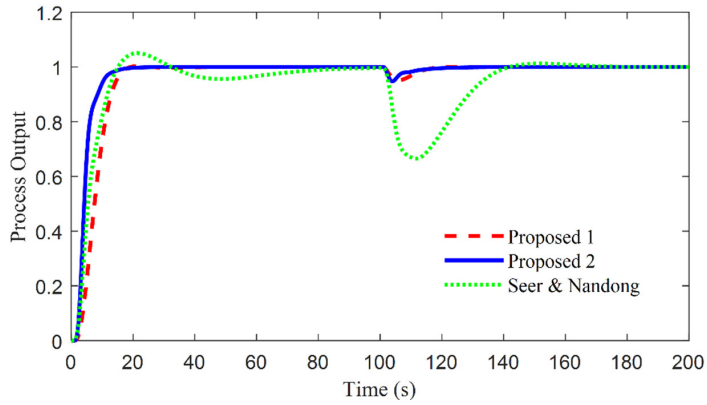

Figure 10: Process output of Example 3

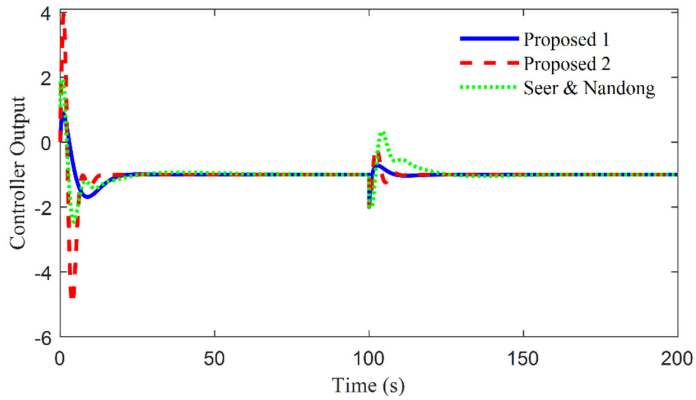

Figure 11: Controller output of Example 3

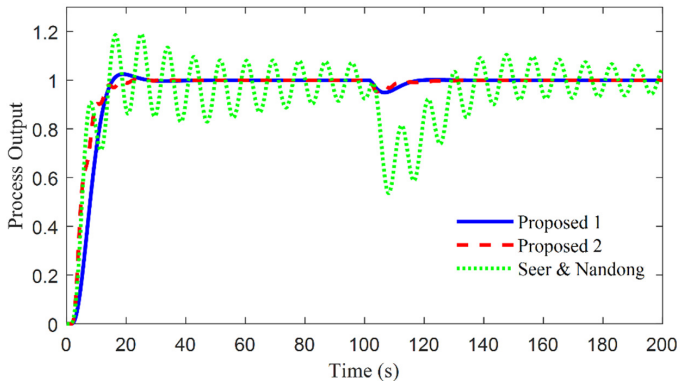

Figure 12: Perturbed process output of Example 3

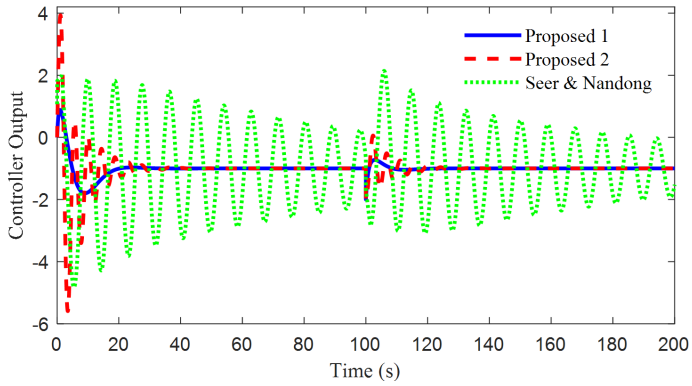

Figure 13: Perturbed controller output of Example 3

Example 4 (A case study on nonlinear chemical reactor)

Fig. 14 presents continuous stirred tank reactor (CSTR) where exothermic chemical reaction takes place. The liquid flowing into the CSTR is same as the liquid flown out.

The following equations describe the process model of CSTR with cooling jacket.

$$\frac{dC_a}{dt} = \frac{F}{V}\left(C_{af} - C_a\right) - k_0 \exp\left(\frac{-E_A}{RT}\right) C_a\,, \tag{27}$$

$$\frac{dT}{dt} = \frac{F}{V}\left(T_f - T\right) + \left(\frac{-\Delta H}{\rho C_p}\right) k_0 \exp\left(\frac{-E_A}{RT}\right) C_a - \frac{UA_r}{V\rho C_p}\left(T - T_j\right), \tag{28}$$

$$\frac{dT_j}{dt} = \frac{F_{jf}}{V_j}\left(T_{jf} - T_j\right) + \frac{UA_r}{V_j \rho_j C_{pj}}\left(T - T_j\right). \tag{29}$$

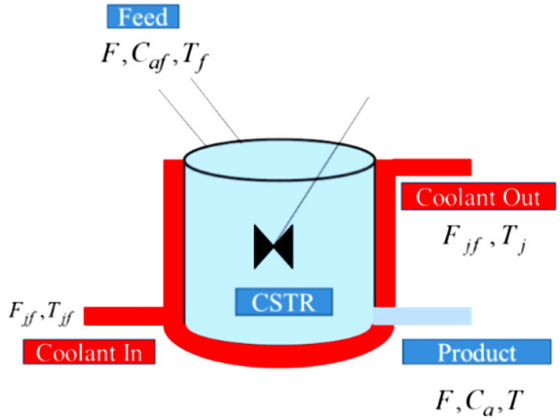

Figure 14: A jacketed CSTR

Here, the concentration of reactant is C_a, F is the rate of feed, the volume of the CSTR is V, C_{af} is the feed concentration, k_0 denotes frequency factor, E_A symbolises energy of activation, the ideal gas-constant is denoted by$R$, the temperature of the CSTR is shown by T, T_f is the feed temperature, H denotes the heat reaction, ρ symbolises the density, C_p is the specific-heat capacity, the heat-transfer coefficient is denoted by U, $A_r$is the area of heat-transfer and T_j denotes the jacket-temperature, F_{jf} is the jacket make-up flow-rate, V_j is the jacket volume, T_{jf} is the coolant inlet temperature, ρ_j is density of the jacket and C_{pj} is the specific heat of jacket. To find the CSTR transfer function, the following state model is used

$$\begin{aligned} \dot{x} &= Ax + Bu, \\ y &= Cx + Du, \end{aligned} \tag{30}$$

in which x is the state variable, u and y are inputs and outputs variables, respectively. The CSTR state model is given by:

$$\begin{aligned} x &= \begin{bmatrix} x_1 \\ x_2 \\ x_3 \end{bmatrix} = \begin{bmatrix} C_a - C_{as} \\ T - T_s \\ T_j - T_{js} \end{bmatrix}, \\ u &= \begin{bmatrix} u_1 \\ u_2 \end{bmatrix} = \begin{bmatrix} F_{jf} - F_{jfs} \\ T_{jf} - T_{jfs} \end{bmatrix}, \\ y &= \begin{bmatrix} y_1 \\ y_2 \end{bmatrix} = \begin{bmatrix} T - T_s \\ T_j - T_{js} \end{bmatrix}. \end{aligned} \tag{31}$$

To get the linear model of the CSTR, these equations are linearized at the steady state values indicated by the subscript 's'. The transfer function of CSTR is found from below relationship

$$G(s) = C(sI - A)^{-1}B + D. \tag{32}$$

In this paper, the CSTR model used is taken from Siddiqui *et al.* [4]. The detailed process modelling of the CSTR may be found in [4]. By comparing above equations with general state equations of a system with the values of operating parameters and steady-state values from Table 3, transfer function of CSTR is found to be

$$\begin{aligned} G(s) = \frac{T(s)}{F_{jf}(s)} &= \frac{-37.94}{1.147s^3 + 10.87s^2 + 21.12s - 34.28} \\ &= \frac{-37.94}{(s - 1.024)\{s - (-5.25 + 1.26i)\}\{s - (-5.25 - 1.26i)\}}. \end{aligned} \tag{33}$$

The transfer function in Eq. (33) has one unstable pole at +1.024 and two stable poles at $-5.25 \pm 1.26i$. The controller is designed for the this unstable CSTR model by Siddiqui *et al.* [4] using their method and from the proposed IMC-SMC technique with PID, and the control parameters are found to be ($k_1 = 18.66$, $k_2 = 23.5$, $k_3 = 9.35$, $K_D = 199.12$ and $\delta = 112.2$) and ($k_1 = -4.1$, $k_2 = -4.1$, $k_3 = -3.5$, $K_D = 4.57$ and $\delta = -4.2$), respectively. The CSTR process model is simulated with these controller settings and tested for a set-point reference of 101.1°F at $t = 0$ s. The disturbance change in T_{jf} from 0°F to 40°F and T_f from 60°F to 80°F are given at $t = 20$ s and at $t = 40$ s, respectively. Fig. 15 and Fig. 16

Table 3: Operating parameters and steady-state values

Parameter	Value	Parameter	Value
C_{af}	0.132 lbmol/ft^3	ρC_p	53.25 Btu/ft^2°F
k_0	16.96×10^{12} h^{-1}	R	1.987 Btu/lbmol °F
E_a	32400 Btu/lbmol	F	340 ft^3/h
V/F	0.25 h	T_f	60°F
$-H$	39 000 Btu/lbmol	V	85 ft^3
UA_r	6600 Btu/h °F	T_s	101.4°F
$\rho_j C_{pj}$	55.6 Btu/ft^3 °F	V_j/V	0.25
T_{jf}	0°F	C_{as}	0.066 lbmol/ft^3
F_{jf}	800 ft^3/h		

Table 4: Performance indices of CSTR

Method	Nominal system					+50% Perturbed system				
	IAE	*ISE*	*ITAE*	*TV*	*IAE* improvement (%)	*IAE* improvement (%)	*ISE*	*ITAE*	*TV*	*IAE* improvement (%)
Siddiqui *et al.* [4]	85.66	2697	2835	2177	149.95	117.6	4048	2903	2008.2	64.93
Shamsuzzoha [40]	209.2	4997	9944	178.1	510.44	209.2	6128	9860	165.5643	193.41
Jeng [41]	91.34	3322	3150	229.9	166.54	149.7	5499	4519	352.2202	109.9
Proposed	**34.27**	**619.2**	**1504**	1649	–	**71.3**	**1299**	**2834**	1 521.1	–

display the responses for temperature of CSTR and jacket make-up flowrate. It is observed from figures that the suggested technique outperforms the other authors' responses with the least overshoot and fast settling point. Also the jacket inlet temperature T_{jf} and feed temperature T_f is well rejected by the suggested technique as compared to the results of Siddiqui *et al.* [4], Shamsuzzoha [40] and Jeng [41]. Table 4 displays the *IAE, ISE, ITAE* and *TV* performance indices. The *IAE* improvement of the suggested controller is compared as per below calculation.

$$IAE \text{ improvement } (\%) = \frac{IAE_{\text{other structure}} - IAE_{\text{proposed SMC}}}{IAE_{\text{proposed SMC}}} \times 100. \qquad (34)$$

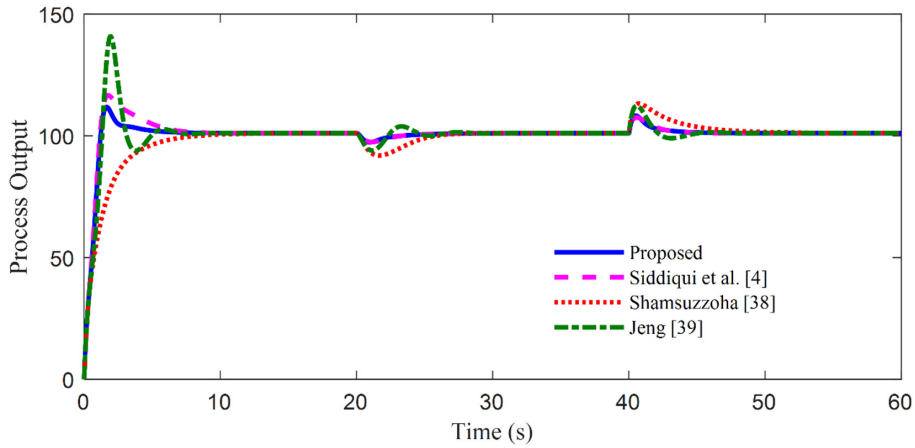

Figure 15: Temperature response of CSTR

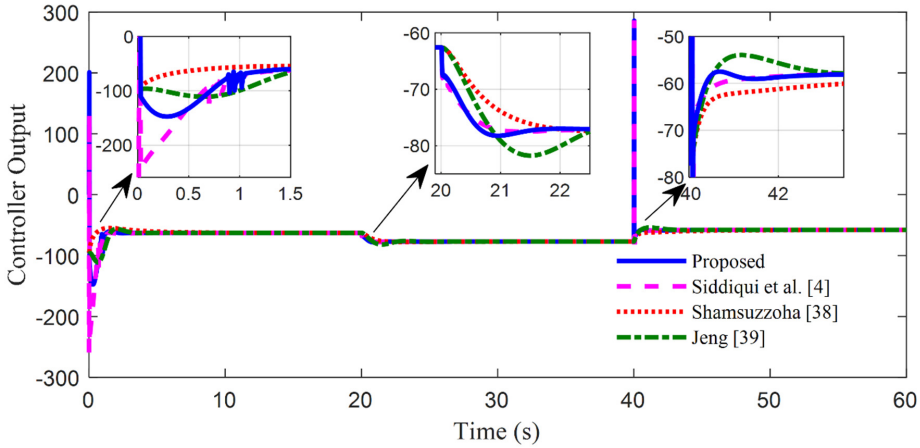

Figure 16: Jacket make-up flowrate response

The least values of these indices show the efficacy of the suggested controller. The *IAE* improvement of the suggested technique is the best over Shamsuzzoha [40] and the least over Siddiqui *et al.* [4].

For the robustness analysis of the proposed technique, perturbation of 50% in the densities, area, specific heat capacities, volumes and heat transfer coefficient of CSTR is introduced and simulated with same controller settings. The perturbed responses are displayed in Fig. 17 and Fig. 18. It is obvious from the response that the suggested controller proves to be highly capable to control the nonlinear CSTR under perturb conditions. The *IAE, ISE* and *ITAE* values in perturbed

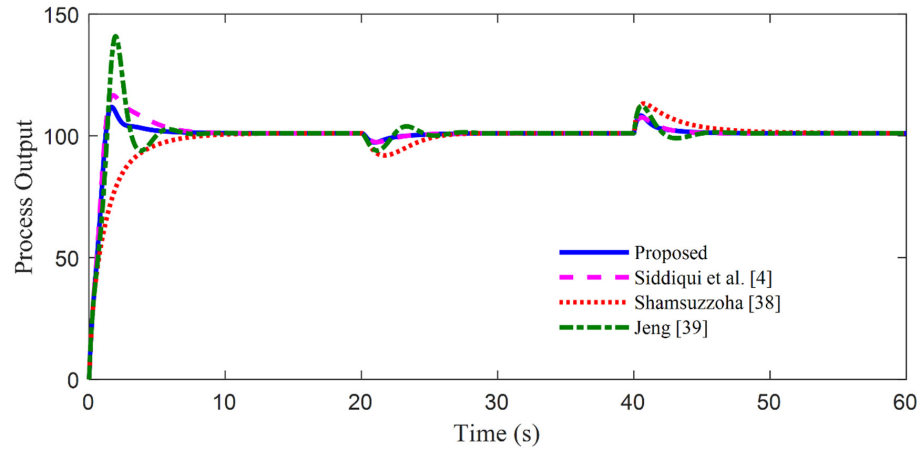

Figure 17: Temperature response of CSTR for +50% perturbation

condition for the suggested technique are the least among others' values which shows the best robustness to the parametric variations.

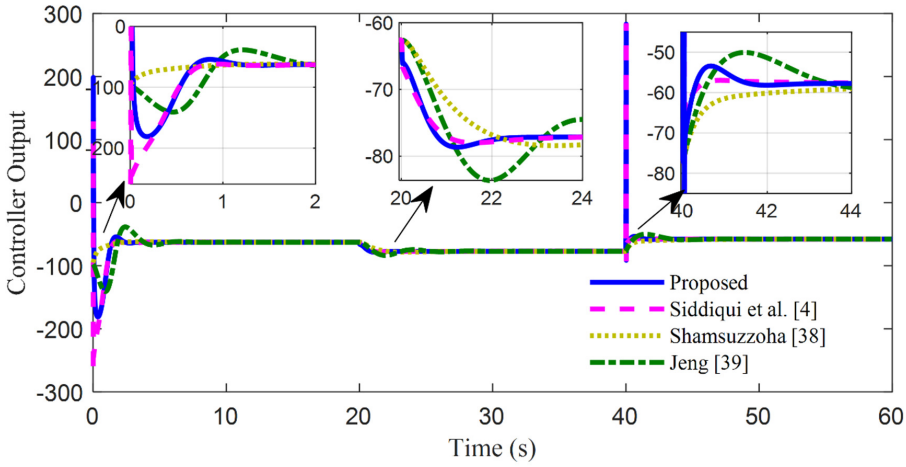

Figure 18: Jacket make-up flowrate response with +50% perturbation

5. Conclusions

In this paper, an IMC based two SMC schemes for unstable SOPDT has been presented. Two different sliding surfaces based on PID and PIDPI are developed for IMC-SMCr for set-point tracking and load disturbance rejection. The parameters for sliding mode controller are obtained using D-E optimization technique by minimising an objective function consisting *IAE* and *TV*. The simulation of different examples is done by the proposed methods and results are effective under different load-disturbances and parameter variations. The effectiveness of the proposed method for temperature control in a CSTR during a first-order irreversible heat-emitting process is also shown. Furthermore, the suggested techniques are found to have lower integral errors *IAE, ISE, ITAE* and *TV* values than the previously published methods in the literature. This approach may be extended to unstable processes with zeros and unstable higher order processes.

List of abbreviations

CSTR	Continuously stirred tank reactor
D-E	Differential Evolution
FOPDT	First order plus dead time
IAE	Integral of absolute error
IMC	Internal model control

IMC-SMCr	Internal model control based sliding mode controller
ISE	Integral of squared error
ITAE	Integral of time absolute error
LD	Load disturbance
PID	Proportional integral derivative
PIDPI	Proportional integral derivative proportional integral
PIDD	Proportional integral derivative derivative
PIDPI	Proportional integral derivative proportional integral
SMC	Sliding mode control
SMCr	Sliding mode controller
SOPDT	Second order plus dead time
SP	Smith predictor
TV	Total variation

References

[1] M. Morari and E. Zafiriou: *Robust Process Control*. Prentice Hall, 1989.

[2] B. Cajamarca, K. Patino, O. Camacho, D. Chavez, P. Leica and M. Pozo: A comparative analysis of sliding mode controllers based on internal model for a nonminimum phase buck and boost converter. *Proceedings of the 2019 International Conference on Information Systems and Computer Science (INCISCOS)*, Quito, Ecuador, (2019), 189–195, DOI: 10.1109/INCISCOS49368.2019.00038

[3] M. Herrera, O. Camacho, H. Leiva and C. Smith: An approach of dynamic sliding mode control for chemical processes. *Journal of Process Control*, **85** (2020), 112–120, DOI: 10.1016/j.jprocont.2019.11.008

[4] M.A. Siddiqui, M.N. Anwar and S.H. Laskar: Control of nonlinear jacketed continuous stirred tank reactor using different control structures. *Journal of Process Control*, **108** (2021), 112–124. DOI: 10.1016/j.jprocont.2021.11.005

[5] J. Espin, F. Castrillon, H. Leiva and O. Camacho: A modified Smith predictor based – Sliding mode control approach for integrating processes with dead time. *Alexandria Engineering Journal*, **61** (2022), 10119–10137. DOI: 10.1016/j.aej.2022.03.045

[6] L. Morales, J.S. Estrada, M. Herrera, A. Rosales, P. Leica and S. Gamboa: Hybrid approaches-based sliding-mode control for pH process control. *ACS Omega*, **7** (2022), 45301–45313. DOI: 10.1021/acsomega.2c05756

[7] Z. Sun, H. Xie, J. Zheng, Z. Man and D. He: Path-following control of Mecanum-wheels omnidirectional mobile robots using nonsingular terminal sliding mode. *Mechanical Systems and Signal Processing*, **147** (2021), DOI: 10.1016/j.ymssp.2020.107128

[8] I. Kaya: Sliding-mode control of stable processes. *Industrial and Engineering Chemistry Research*, **46**(2), (2007), 571–578. DOI: 10.1021/ie0607806

[9] M.A. Siddiqui, M.N. Anwar and S.H. Laskar: Sliding mode controller design for second-order unstable processes with dead-time. *Journal of Electrical Engineering*, **71**(4), (2020), 237–245. DOI: 10.2478/jee-2020-0032

[10] A. Li, M. Liu and Y. Shi: Adaptive sliding mode attitude tracking control for flexible spacecraft systems based on the Takagi-Sugeno fuzzy modelling method. *Acta Astronautica*, **175** (2020), 570–581. DOI: 10.1016/j.actaastro.2020.05.041

[11] J. Long, S. Zhu, P. Cui and Z. Liang: Barrier Lyapunov function based sliding mode control for Mars atmospheric entry trajectory tracking with input saturation constraint. *Aerospace Science and Technology*, **106** (2020), DOI: 10.1016/j.ast.2020.106213

[12] P. Mani and Y.H. Joo: Fuzzy logic-based integral sliding mode control of multi-area power systems integrated with wind farms. *Information Sciences*, **545** (2021), 153–169, DOI: 10.1016/j.ins.2020.07.076

[13] M.A. Ebrahim, M.N. Ahmed, H.S. Ramadan, M. Becherif and J. Zhao: Optimal metaheuristic-based sliding mode control of VSC-HVDC transmission systems. *Mathematics and Computers in Simulation*, **179** (2021), 178–193, DOI: 10.1016/j.matcom.2020.08.009

[14] L.Y. Hao, H. Zhang, H. Li and T.S. Li: Sliding mode fault-tolerant control for unmanned marine vehicles with signal quantization and time-delay. *Ocean Engineering*, **215** (2020), DOI: 10.1016/j.oceaneng.2020.107882

[15] X. Liu, M. Zhang, J. Chen and B. Yin: Trajectory tracking with quaternion-based attitude representation for autonomous underwater vehicle based on terminal sliding mode control. *Applied Ocean Research*, **104** (2020), DOI: 10.1016/j.apor.2020.102342

[16] Y. Islam, I. Ahmad, M. Zubair and K. Shahzad: Double integral sliding mode control of leukemia therapy. *Biomedical Signal Processing and Control*, **61** (2020), DOI: 10.1016/j.bspc.2020.102046

[17] S. Rezvani-Ardakani, S. Mohammad-Ali-Nezhad and R. Ghasemi: Epilepsy control using a fixed time integral super twisting sliding mode control for Pinsky–Rinzel pyramidal model through ion channels with optogenetic method. *Computer Methods and Programs in Biomedicine*, **195** (2020), DOI: 10.1016/j.cmpb.2020.105665

[18] U. Mehta and I. Kaya: Smith predictor with sliding mode control for processes with large dead times. *Journal of Electrical Engineering*, **68**(6), (2017), 463–469, DOI: 10.1515/jee-2017-0081

[19] O. Camacho and C. A. Smith: Sliding mode control: An approach to regulate nonlinear chemical processes. *ISA Transactions*, **39**(2), (2000), 205–218, DOI: 10.1016/s0019-0578(99)00043-9

[20] R. Rojas, O. Camacho and L. González: A sliding mode control proposal for open-loop unstable processes. *ISA Transactions*, **43**(2), (2004), 243–255, DOI: 10.1016/s0019-0578(07)60034-2

[21] O. Camacho and F. De la Cruz: Smith predictor based-sliding mode controller for integrating processes with elevated deadtime. *ISA Transactions*, **43**(2), (2004), 257–270, DOI: 10.1016/s0019-0578(07)60035-4

[22] D.B. Talange, A.R. Laware and V.S. Bandal: Development of an internal model sliding mode controller for cascade control system. *Proceedings of 2015 International Conference on Energy Systems and Applications*, Pune, India, (2016), 51–56, DOI: 10.1109/ICESA.2015.7503312

[23] M.M.P. De La Parte, O. Camacho and E.F. Camacho: A GPC-based sliding mode controller for nonlinear chemical processes. *Proceedings of the European Control Conference (ECC 2001)*, Porto, Portugal, (2001), 3777–3782, DOI: 10.23919/ecc.2001.7076522

[24] O. Camacho, C. Smith and W. Moreno: Development of an internal model sliding mode controller. *Industrial and Engineering Chemistry Research*, **42**(3), (2003), 568–573, DOI: 10.1021/ie010481a

[25] U. Mehta and R. Rojas: Smith predictor based sliding mode control for a class of unstable processes. *Transactions of the Institute of Measurement and Control*, **39**(5), (2017), 1–9, DOI: 10.1177/0142331215619973

[26] D.B. Talange, A.R. Laware and V.S. Bandal: Development of an internal model sliding mode controller for cascade control system. *Proceedings of the International Conference on Energy Systems and Applications (ICESA 2015)*, Pune, India, (2015), 51–56, DOI: 10.1109/ICESA.2015.7503312

[27] O. Camacho: A predictive approach based-sliding mode control. *IFAC Proceedings Volumes*, **15**(1), (2002), 381–385, DOI: 10.3182/20020721-6-es-1901.00632

[28] O. Camacho and R. Rojas: A general sliding mode controller for nonlinear chemical processes. *Journal of Dynamic Systems, Measurement, and Control*, **122** (2000), 650–655, DOI: 10.1115/1.1318351

[29] R. Storn and K. Price: Differential evolution – A simple and efficient heuristic for global optimization over continuous spaces. *Journal of Global Optimization*, **11**(3), (1997), 341–359, DOI: 10.1023/A:1008202821328

[30] S. Saremi, S. Mirjalili and A. Lewis: Grasshopper optimisation algorithm: Theory and application. *Advances in Engineering Software*, **105** (2017), 30–47, DOI: 10.1016/j.advengsoft.2017.01.004

[31] A.K. Barik and D.C. Das: Expeditious frequency control of solar photovoltaic/biogas/biodiesel generator based isolated renewable microgrid using grasshopper optimisation algorithm. *IET Renewable Power Generation*, **12**(14), (2018), 1659–1667, DOI: 10.1049/iet-rpg.2018.5196

[32] T. Eltaeib and A. Mahmood: Differential evolution: A survey and analysis. *Applied Science*, **8**(10), (2018), DOI: 10.3390/app8101945

[33] S. Skogasted: Simple analytic rules for model reduction and PID controller tuning. *Journal of Process Control*, **13**(4), (2003), 291–309, DOI: 10.1016/S0959-1524(02)00062-8

[34] S. Atic and I. Kaya: PID controller design based on generalized stability boundary locus to control unstable processes with dead time. *Proceedings of the 26th Mediterranean Conference on Control and Automation (MED)*, Zadar, Croatia, (2018) 1–6, DOI: 10.1109/MED.2018.8442568

[35] N. Anwar and S. Pan: A frequency response model matching method for PID controller design for processes with dead-time. *ISA Transactions*, **55**(3), (2014), 175–187, DOI: 10.1016/j.isatra.2014.08.020

[36] A. Raza and M.N. Anwar: A unified approach of PID controller design for unstable processes with time delay. *Journal of Central South University*, **27**(9), (2020), 2643–2661, DOI: 10.1007/s11771-020-4488-6

[37] W. Cho, J. Lee and T.F. Edgar: Simple analytic proportional-integral-derivative (PID) controller tuning rules for unstable processes. *Industrial and Engineering Chemistry Research*, **53**(13), (2014), 5048–5054, DOI: 10.1021/ie401018g

[38] M. Shamsuzzoha and M. Lee: Enhanced disturbance rejection for open-loop unstable process with time delay. *ISA Transactions*, **48**(2), (2009), 237–244, DOI: 10.1016/j.isatra.2008.10.010

[39] Q.H. Seer and J. Nandong: Stabilization and PID tuning algorithms for second-order unstable processes with time-delays. *ISA Transations*, **67** (2017), 233–245, DOI: 10.1016/j.isatra.2017.01.017

[40] M. Shamsuzzoha: Closed-loop PI/PID controller tuning for stable and integrating process with time delay. *Industrial and Engineering Chemistry Research*, **52**(36), (2013), 12973–12992, DOI: 10.1021/ie401808m

[41] J.C. Jeng: Simultaneous closed-loop tuning of cascade controllers based directly on set-point step-response data. *Journal of Process Control*, **24**(5), (2014), 652–662, DOI: 10.1016/j.jprocont.2014.03.007